Supplement of Clim. Past, 19, 1275–1294, 2023
https://doi.org/10.5194/cp-19-1275-2023-supplement

Climate of the Past
Open Access
EGU

Supplement of

Effects of Last Glacial Maximum (LGM) sea surface temperature and sea ice extent on the isotope–temperature slope at polar ice core sites

Alexandre Cauquoin et al.

Correspondence to: Alexandre Cauquoin (cauquoin@iis.u-tokyo.ac.jp)

S1. ECHAM6-wiso sensitivity simulations

Several sets of LGM and PI sensitivity simulations with ECHAM6-wiso have been performed:

- The AMOC variations from MIROC4m LGM and the selected time periods for our ECHAM6-wiso simulations using MIROC 4m sea surface boundary conditions are shown in Figure S1. The maps of LGM-PI anomalies in 2m air temperature, precipitation and $\delta^{18}O_p$ according to our different ECHAM6-wiso are displayed in Figure S2, S3 and S4, respectively. The Figure S6 shows the model-data comparison of $\Delta_{LGM-PI}\delta^{18}O_{sn}$ at polar ice core stations for the strong LGM AMOC case. The annual mean anomalies in vertically integrated water vapor transport and integrated column of water vapor for a stronger cooling in the Admunsen Sea are shown in Figure S7. The same anomalies but for austral winter between more and less extensive sea ice simulations are shown in Figure S8. The average modeled values of $\delta^{18}O_p$-temperature temporal slope for East Antarctic, West Antarctic and Greenland regions according to our different simulations are indicated in Figure S9.

- In ECHAM6-wiso, the isotopic composition of sea ice surfaces also reflects the isotopic composition of snow (PI $\delta^{18}O$ between -5 and -30 ‰) deposited on this surface (Bonne et al., 2019; Cauquoin and Werner, 2021), meaning that sublimation of deposited snow on sea ice influences the isotopic composition of the above surface water vapor. This process leads to a stronger depletion of surface water vapor over sea ice covered areas. We disabled this process in LGM and PI simulations using MIROC 4m SST and sea ice (i.e., LGM_miroc4m_sst_and_sic and the corresponding PI simulations). In this case, the isotopic composition of sea ice surfaces equals the one of the ocean waters just beneath the sea ice, only (i.e., $\delta^{18}O$ around 0 ‰). The impacts on modeled $\delta^{18}O_p$-temperature temporal slopes in polar regions are shown in Figure S10.

- The sea ice area fraction from MIROC 4m is lower in coastal grid cells (see section 2.2.2), especially in the Arctic. To evaluate the impacts of this parameterization on modeled $\delta^{18}O_p$-temperature temporal slopes, LGM and PI sea ice fields from MIROC 4m (from LGM_miroc4m_sst_and_sic and the corresponding PI simulations, see Table 1) are modified in the following way: (1) monthly sea ice area fraction cannot decrease going north (south) in the Northern (Southern) Hemisphere and (2) all monthly sea ice area fraction values above 95 % are set to 100 ‰ (Figure S11). The impacts on modeled $\delta^{18}O_p$-temperature temporal slopes in Greenland region are shown in Figure S12.

- To test if the general bias in modeled $\delta^{18}O$ in Antarctica is due to the GLAC-1D LGM ice sheet reconstruction prescribed for the ECHAM6-wiso simulation, another LGM simulation using the PMIP3 ice sheet reconstruction instead of GLAC-1D has been performed. The PMIP3 ice sheet reconstruction contains stronger elevation changes in Antarctica, especially in the western part of the continent (see Figure 3 of Werner et al., 2018). We used the sea surface boundary conditions from GLOMAP for this simulation. The model-data comparison and the spatial distribution of modeled $\delta^{18}O_p$-temperature temporal slope in Antarctic and Greenland areas are shown in Figure S5 and S13, respectively.

S2. $\delta^{18}O$ SISALv2 speleothem data for LGM and PI

As recommended by Comas-Bru et al. (2019), we defined here averaged PI and LGM values as the means of the 1850-1990 CE and 21 ± 1 ka periods, respectively. To compare the $\delta^{18}O$ of speleothem data with our modeled $\delta^{18}O$ of precipitation, the measured $\delta^{18}O$ of calcite or aragonite are converted into $\delta^{18}O$ of drip-water using equations 1 or 2 of Comas-Bru et al. (2019), respectively, after conversion from V-PDB to VSMOW scale (equation 3 of Comas-Bru et al. (2019)). The annual mean surface air temperature from ECHAM6-wiso is used for the conversion.

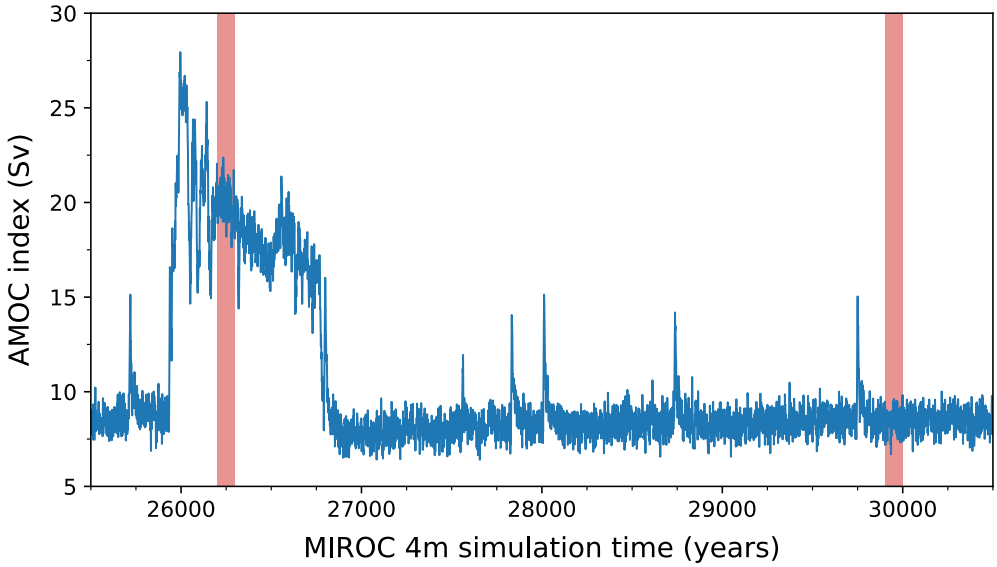

Figure S1: AMOC variations in MIROC 4m LGM simulation. The red rectangles are the 100-year periods selected for the strong and weak AMOC phase.

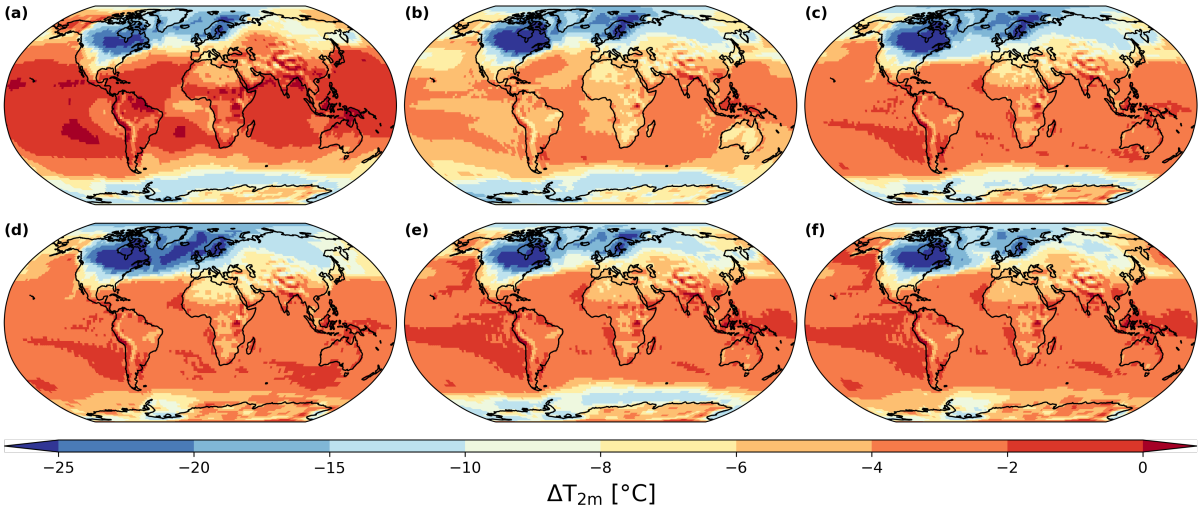

Figure S2: Modeled 2m air temperature anomalies between LGM and PI from our different ECHAM6-wiso simulations: (a) LGM_GLOMAP, (b) LGM_tierney2020, (c) LGM_miroc4m_sst_glomap_sic, (d) LGM_miroc4m_sst_and_sic, (e) LGM_miroc4m_strong_AMOC_sst_glomap_sic, and (f) LGM_miroc4m_strong_AMOC_sst_and_sic.

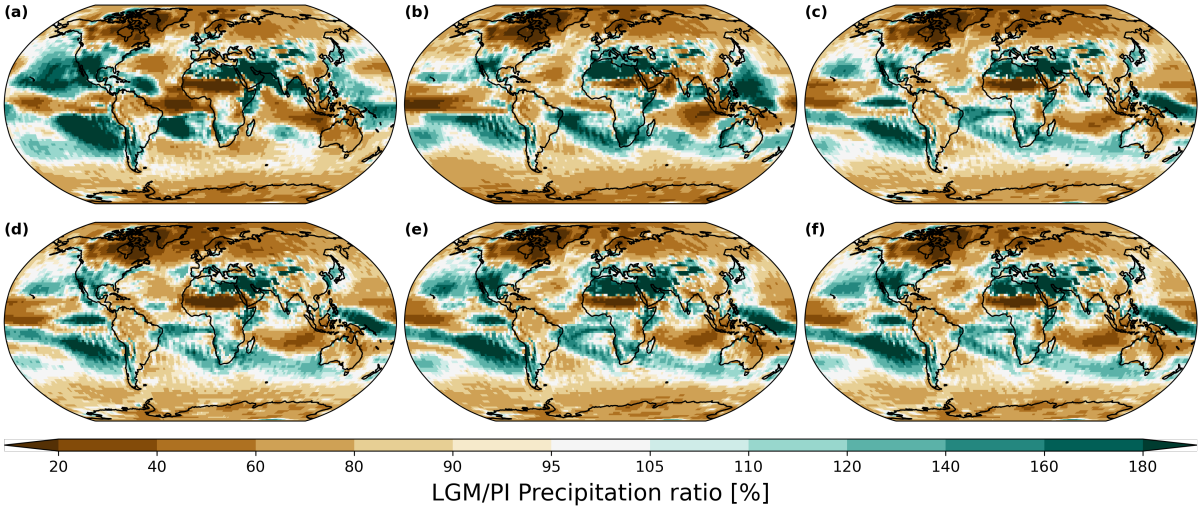

Figure S3: Same as Figure S1 but for modeled LGM/PI precipitation ratios.

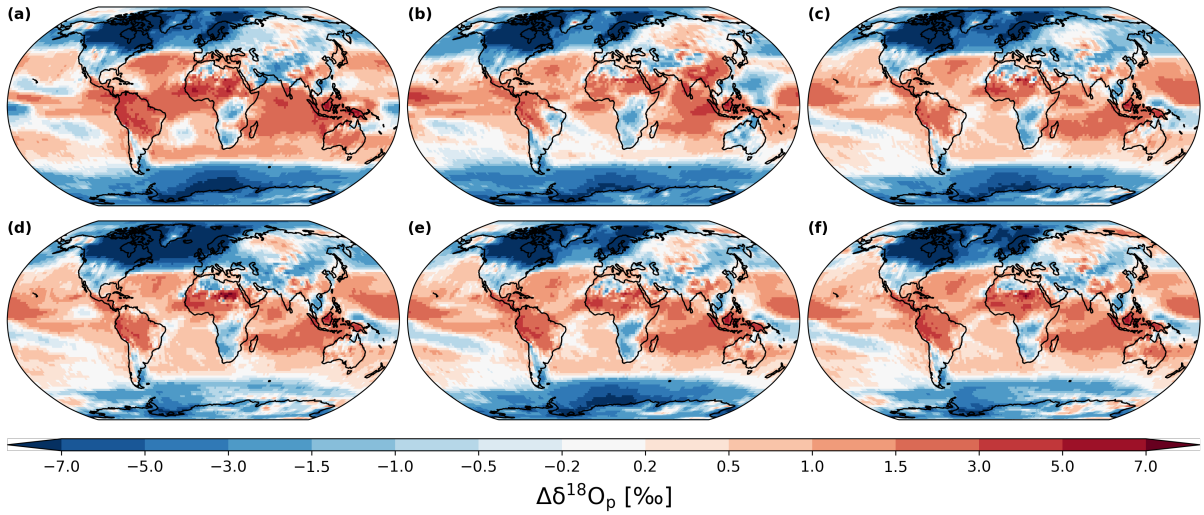

Figure S4: Same as Figure S1 but for modeled $\delta^{18}O_p$ anomalies.

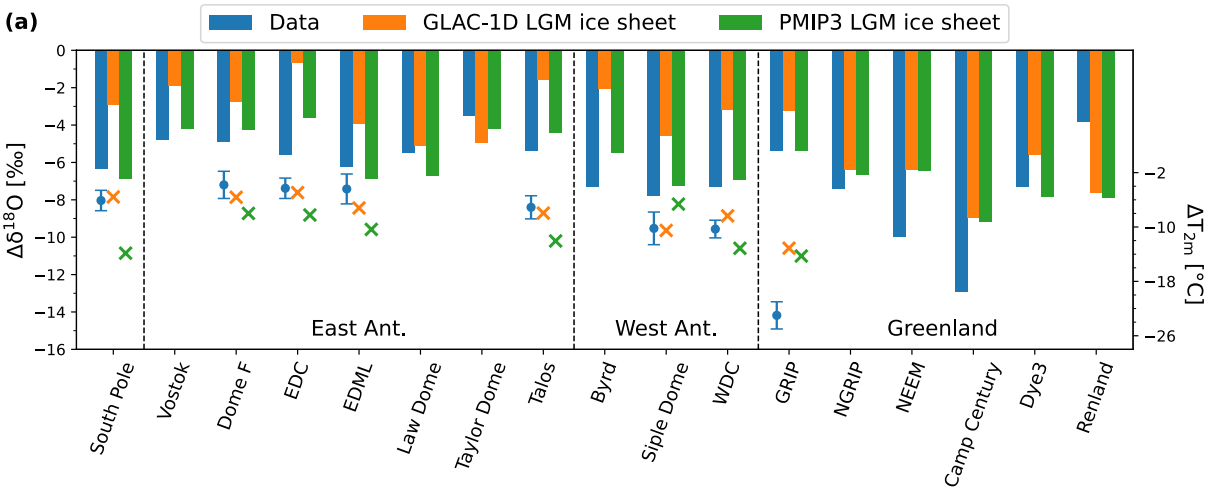

Figure S5: Comparison of $\delta^{18}O$ anomalies measured in polar ice cores (blue bars) with modeled anomalies in $\delta^{18}O_{sn}$ between LGM and PI from ECHAM6-wiso simulations using the PMIP3 LGM ice sheet or GLAC-1D (green and orange bars, respectively). The sea surface boundary conditions are from GLOMAP for the two simulations.

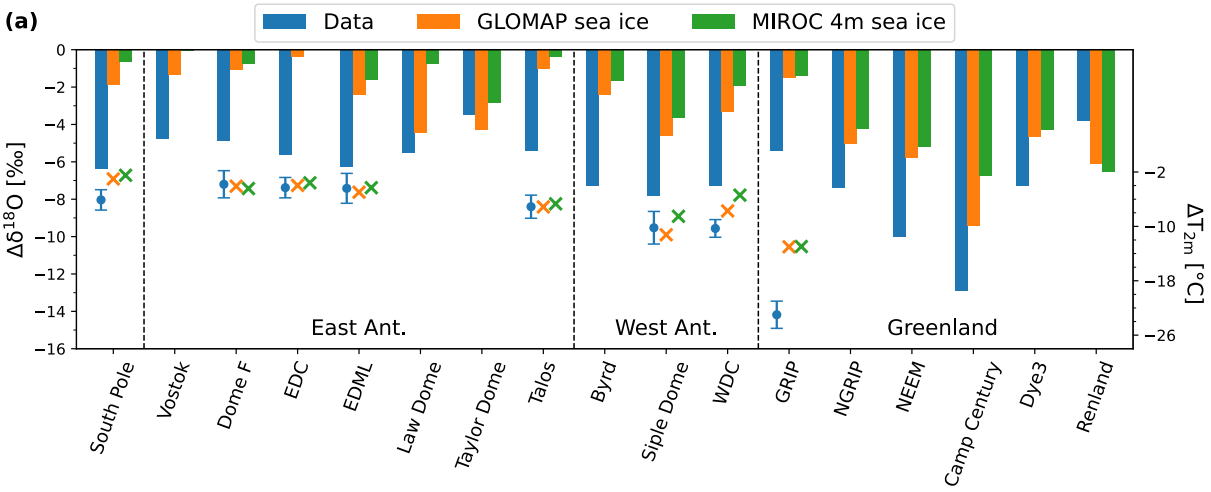

Figure S6: Same as Figure 6a but with SST (green and orange bars) and sea ice (green bars) from MIROC 4m with strong LGM AMOC simulation.

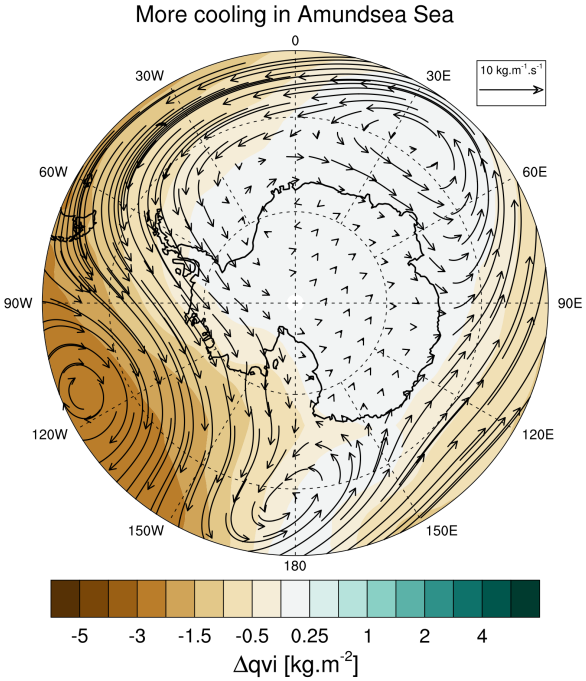

Figure S7: Annual mean anomalies in vertically integrated water vapor transport (arrows) and integrated column of water vapor (colored backgrounds) between more and less cooling in Admunsen Sea (LGM_tierney2020 – LGM_glomap).

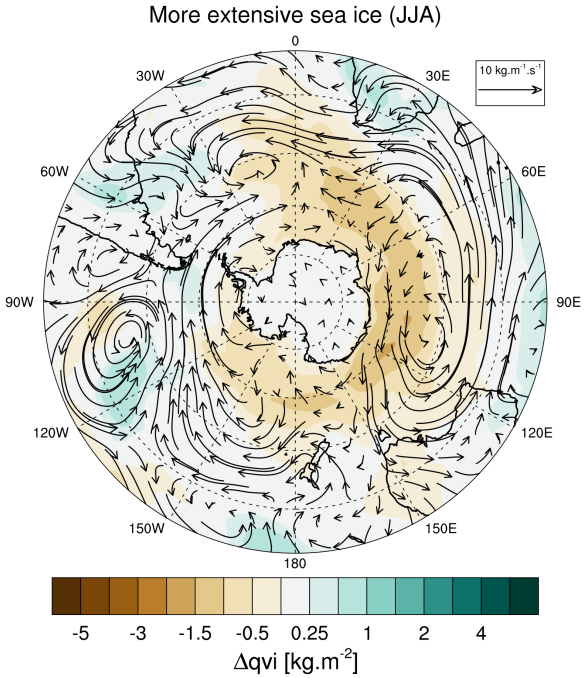

Figure S8: Austral winter (JJA) anomalies in vertically integrated water vapor transport (arrows) and integrated column of water vapor (colored backgrounds) between more and less extended sea ice simulations (LGM_miroc4m_sst_glomap_sic – LGM_miroc4m_sst_and_sic).

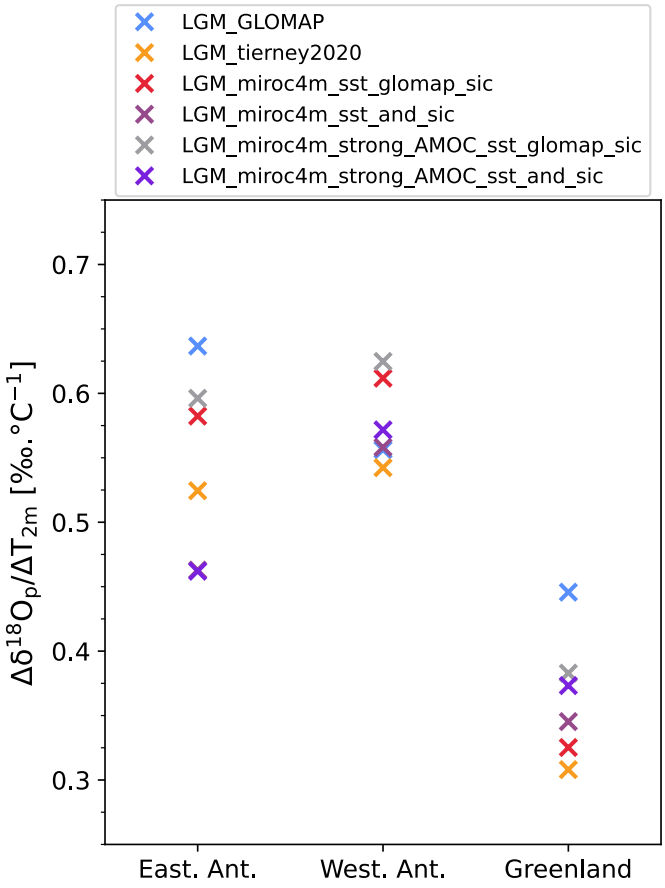

Figure S9: Average modeled values of $\delta^{18}O_p$-temperature temporal slope for East Antarctic, West Antarctic and Greenland regions according to our different simulations.

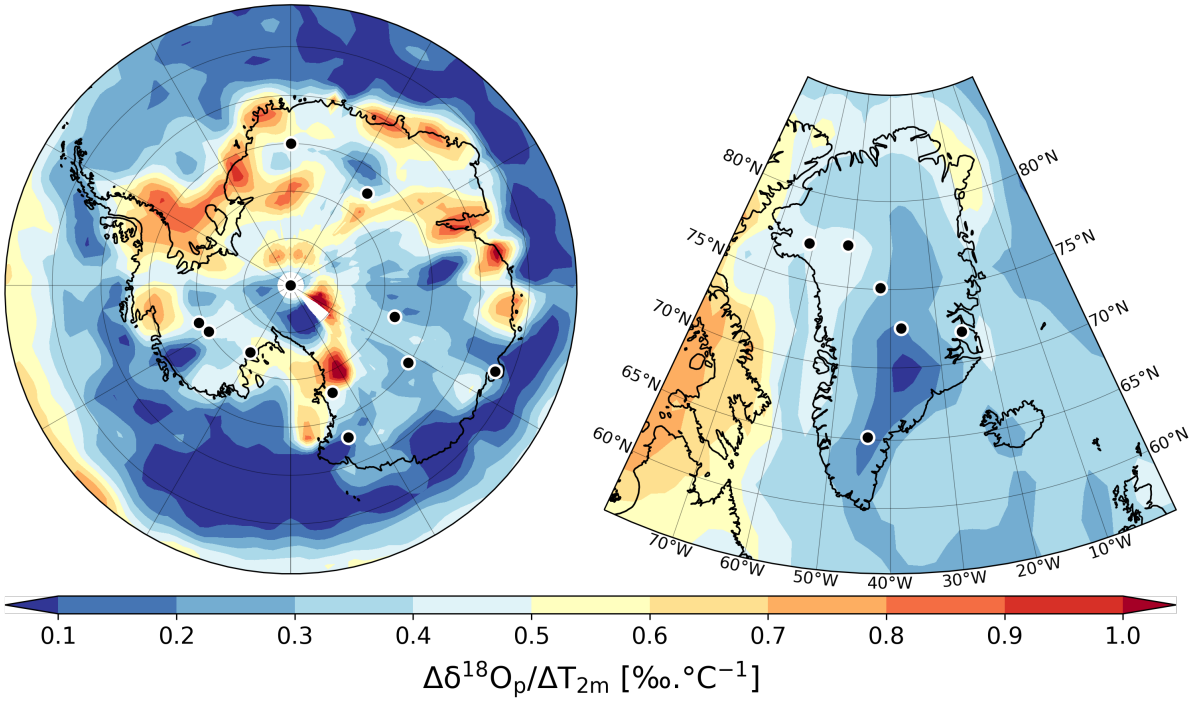

Figure S10: Spatial distribution of $\delta^{18}O_p$-temperature temporal slope in Antarctic and Greenland areas (left and right plots, respectively) for LGM-PI changes using the same sea surface boundary conditions as in LGM_miroc4m_sst_and_sic simulation, but without taking into account the isotopic content of snow on sea ice for sublimation processes in sea ice covered regions (see Text S1).

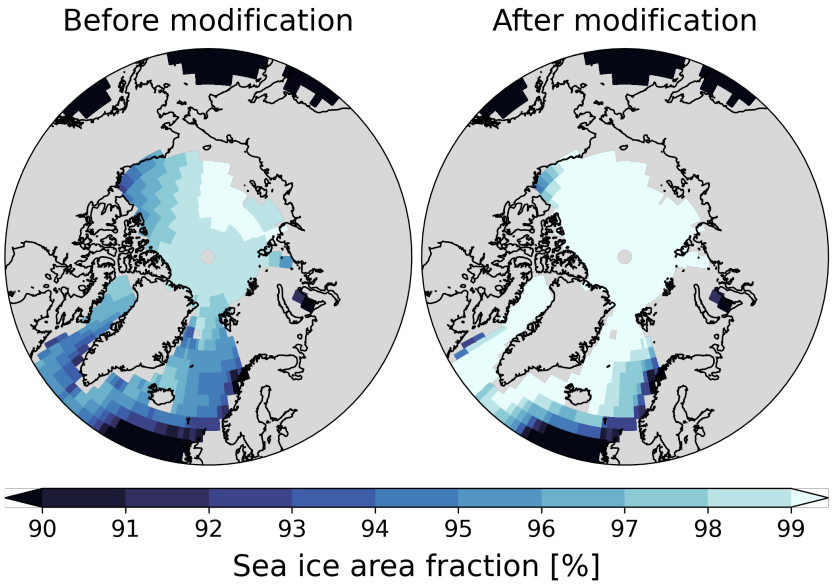

Figure S11: Mean LGM sea ice area fraction from MIROC 4m (LGM_miroc4m_sst_and_sic simulation) before and after the modifications described in the Supplementary Text S1.

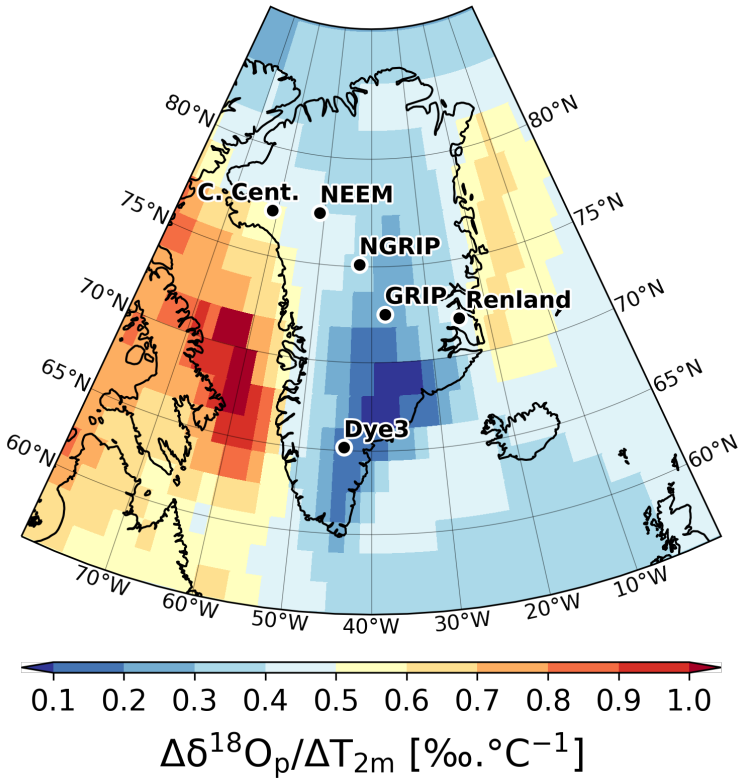

Figure S12: Spatial distribution of $\delta^{18}O_p$-temperature temporal slope in Greenland area for LGM-PI changes using the modified sea ice field boundary conditions shown in Figure S8 (see Text S1 for details).

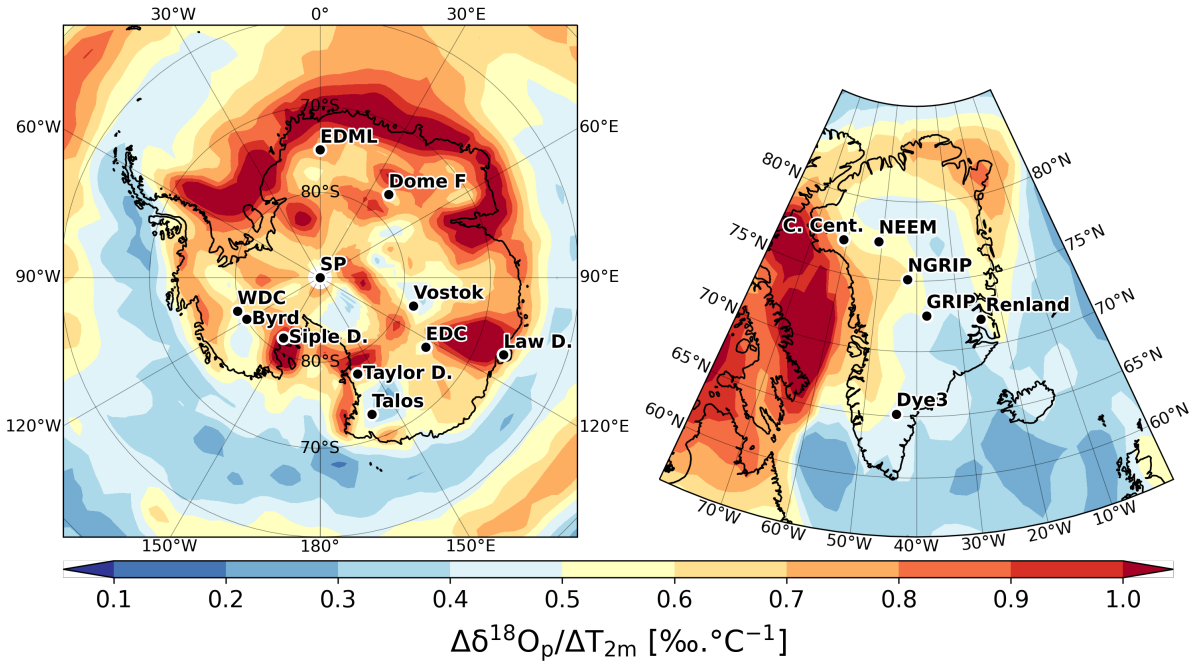

Figure S13: Spatial distribution of $\delta^{18}O_p$-temperature temporal slope in Antarctic and Greenland areas (left and right plots, respectively) for LGM-PI changes using the PMIP3 LGM ice sheet reconstruction instead of GLAC-1D.

References

Bonne, J.-L., Behrens, M., Meyer, H., Kipfstuhl, S., Rabe, B., Schönicke, L., Steen-Larsen, H. C., and Werner, M.: Resolving the controls of water vapour isotopes in the Atlantic sector, Nat. Commun., 10, 1632, https://doi.org/10.1038/s41467-019-09242-6, 2019.

Cauquoin, A. and Werner, M.: High-Resolution Nudged Isotope Modeling With ECHAM6-Wiso: Impacts of Updated Model Physics and ERA5 Reanalysis Data, J. Adv. Model. Earth Syst., 13, https://doi.org/10.1029/2021MS002532, 2021.

Comas-Bru, L., Harrison, S. P., Werner, M., Rehfeld, K., Scroxton, N., Veiga-Pires, C., and SISAL working group members: Evaluating model outputs using integrated global speleothem records of climate change since the last glacial, Clim. Past, 15, 1557–1579, https://doi.org/10.5194/cp-15-1557-2019, 2019.

Werner, M., Jouzel, J., Masson-Delmotte, V., and Lohmann, G.: Reconciling glacial Antarctic water stable isotopes with ice sheet topography and the isotopic paleothermometer, Nat. Commun., 9, https://doi.org/10.1038/s41467-018-05430-y, 2018.